α-Oxyiminophosphonates: Chemical and Physical Properties. Reactions, Theoretical Calculations, and *X*-Ray Crystal Structures of (*E*) and (*Z*)-Dimethyl α-Hydroxyiminobenzylphosphonates

Eli Breuer,* Rafik Karaman, Amiram Goldblum, and Dan Gibson
Department of Pharmaceutical Chemistry, The Hebrew University School of Pharmacy, Jerusalem, Israel
Haim Leader
The Israel Institute for Biological Research, Ness Ziona, Israel
Barry V. L. Potter and Jane H. Cummins
The Department of Chemistry, Leicester University, Leicester

Dialkyl α-oxyiminoalkylphosphonates, obtained by treatment of dialkyl acylphosphonates with hydroxylamine or methoxylamine, are mostly mixtures of *E* and *Z* isomers. Structural assignments of the oximes were based on *X*-ray crystallographic analysis of representative compounds: (*E*)- and (*Z*)-dimethyl α-hydroxyiminobenzylphosphonates [(*E*)- and (*Z*)-(**1a**)]. The ^{31}P n.m.r. chemical shifts of the *E* isomers always appear at lower field than those of the corresponding *Z* isomers. Thermal fragmentation of (**1a**) affords benzonitrile and dimethyl hydrogen phosphate, with (*Z*)-(**1a**) reacting faster than the *E* isomer. α-Oxyiminophosphonates undergo $E \rightleftharpoons Z$ isomerization catalysed either by acid or by base under certain conditions, the *E* isomer being the thermodynamically more stable one. An *E* + *Z* mixture of dialkyl α-oxyiminophosphonates can be mono-de-alkylated by non-basic nucleophiles (*e.g.* NaI) to afford monoalkyl oxyiminophosphonates of unchanged isomeric composition. The geometrical isomers of α-hydroxyiminophosphonates differ in their behaviour under basic conditions. While treatment of (*E*)-(**1a**) with NaOH in boiling methanol leads, by mono-de-alkylation, to sodium methyl α-hydroxyiminobenzylphosphonate [(*E*)-(**2a**)], under the same conditions (*Z*)-(**1a**) undergoes fragmentation, by C–P bond cleavage, to benzonitrile and dimethyl hydrogen phosphate. Control experiments established that the fragmentation of (*Z*)-α-hydroxyiminophosphonates involves an intramolecular attack on the phosphorus atom by the ionized *Z* oriented oxime oxygen. Similar differences in behaviour are noted between the isomers of the monoanions of α-hydroxyiminophosphonates. MNDO/H Calculations demonstrate the feasibility of forming internal hydrogen bonds in *Z* isomers, and their possible contribution to conformational preferences. Single-crystal *X*-ray diffraction studies of (*E*)- and (*Z*)-(**1a**), and (*E*)-(**2b**), clearly identified the geometric isomers and correlated them with the ^{1}H and ^{31}P n.m.r. resonances.

While dialkyl α-oxyiminophosphonates [*e.g.* (**1**)[1]] are readily available from acylphosphonates,[2] their chemistry and that of the corresponding hydroxyiminophosphonic acids and monoesters [*e.g.* (**2**)] is almost completely unexplored, apart from their use as starting materials for the synthesis of α-aminophosphonic acids.[3] We consider this group of compounds worthy of interest, because the combination of the oxime and phosphonic functions provides a new type of bifunctional group that can reasonably be expected to possess interesting metal-binding properties.†

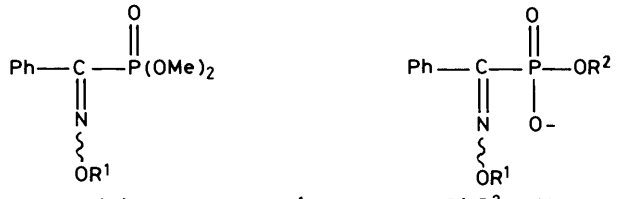

Furthermore such a hydroxyiminophosphonic functionality can easily be incorporated into virtually any type of organic molecule that has, or may be attached to, a carboxy group (*e.g.* peptide, steroid, polymer *etc.*) thus allowing the design of molecules with potential biological or technological importance.

The present paper describes the results of our studies concerning the preparation, structure, and the reactivity of simple dialkyl α-hydroxyiminophosphonates and their monoesters. For these studies we chose the oximes of benzoylphosphonates and their derivatives as representative compounds of this class.‡

We have recently reported that such monoesters act as phosphorylating agents for alcohols, as they can serve as sources for the generation of monomeric methyl metaphosphate,[4] and that α-hydroxyiminophosphonic diacids undergo fragmentation by a dissociative mechanism involving the intermediacy of monomeric metaphosphate anion.[5]

Results and Discussion

Preparation and Structure of Dialkyl α-Hydroxyiminophosphonates.—Dialkyl α-hydroxyiminophosphonates were first obtained by Berlin by reaction of dialkyl acylphosphonates[2] with hydroxylamine.[1] The use of Berlin's method for the preparation of α-hydroxyiminophosphonates in our hands also proved to be a reliable procedure, which yielded the desired compounds usually in high (>80%) yields. Examination of the products obtained by ^{31}P n.m.r. spectroscopy revealed that

† D. Gibson, *et al.*, manuscript in preparation.
‡ The physical constants of a series of other α-hydroxyiminoalkylphosphonates prepared are described in the Experimental section.

Table 1. ^{31}P-N.m.r. chemical shifts of compounds (**1**) and (**2**)

Compound	*E* δ_P	*Z* δ_P	Solvent
(**1a**)	11.60[a]	5.18[a]	$CDCl_3$
(**1b**)	10.12	5.68	$CDCl_3$
(**2a**)·Na^+	6.43	1.83	D_2O
(**2b**)·Na^+	6.43[a]	1.64	D_2O

[a] Structure by *X*-ray crystallography.

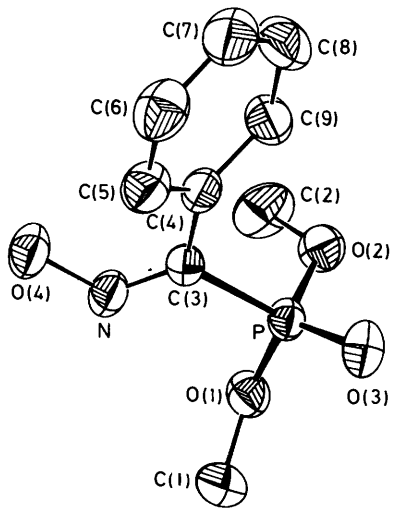

Figure 1. Structure of (*E*)-(**1a**), showing 50% probability thermal ellipsoids and atom-labelling scheme

in most cases * the product was composed of two isomeric oximes [$\Delta\delta$ ^{31}P 4—6 p.p.m. in $CDCl_3$). In contrast, ^{1}H n.m.r. spectroscopy was not always useful as a diagnostic tool for revealing the presence of two isomers. However in those cases in which the two isomers were distinguishable, the P–O–Me proton signal of the *E* isomer always appeared at lower field, by *ca.* 0.05—0.08 p.p.m., than the corresponding signal of the *Z* isomer.

Structural assignments of the isomeric oximes are based upon single-crystal *X*-ray crystallographic analyses of (*E*)- and (*Z*)-dimethyl α-hydroxyiminophosphonate [(*E*)-(**1a**)], [(*Z*)-(**1a**)] and of (*E*)-sodium methyl α-methoxyiminophosphonate [(*E*)-(**2b**)·Na^+]† which were obtained in crystalline form. In all of these cases the *E* isomer resonated at lower field in the ^{31}P n.m.r. spectrum (See Table 1). This is consistent with the expected shielding effect of the phosphorus by the lone pairs of the oxime oxygen.[6] As a consequence the *E* isomers are expected to resonate at lower field than the corresponding *Z* isomers. On this basis the *E* structures are assigned to the lower-field components of all pairs of isomers obtained and for which no *X*-ray data are available.

* Since the procedure for the preparation of dialkyl oxyiminophosphonates involves acidic treatment during the work-up, and since we found that $Z \longrightarrow E$ isomerization is catalysed by acid, the *E*/*Z* ratio of products actually obtained in the various cases is somewhat incidental. In some cases only one product (presumably *E*) was obtained, probably due to fast $Z \longrightarrow E$ isomerization.

† The unit-cell parameters of *E*-(**2b**) are given in Table 12. A comprehensive structural analysis of this molecule will be published elsewhere.

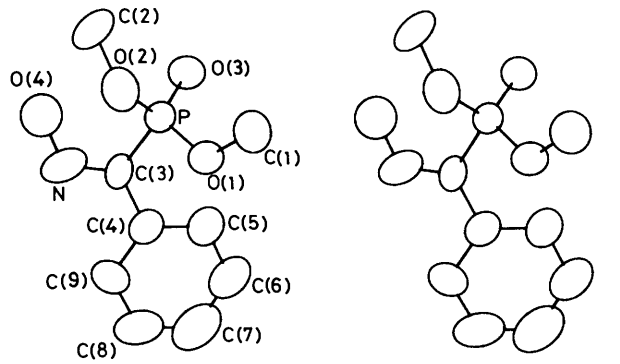

Figure 2. A stereoview of (*Z*)-(**1a**)-I, depicting the molecular geometry as well as the labelling scheme

Final non-hydrogen positional parameters, together with their estimated standard deviations for both structures [(*E*)-(**1a**) and (*Z*)-(**1a**), appear in Table 2. Important interatomic distances and bond angles, together with their standard deviations, are given in Table 3, and the torsional angles are listed in Table 4. Figure 1 depicts the geometry and the labelling scheme for (*E*)-(**1a**) and Figure 2 displays a stereoview and the labelling scheme for molecule 1 of (*Z*)-(**1a**), [(*Z*)-(**1a**)-I). (There are two independent molecules [(*Z*)-(**1a**)-I and (*Z*)-(**1a**)-II] in the asymmetric unit.)

Thermal Fragmentation of Dimethyl α-Oxyiminobenzylphosphonates (**1a**) *and* (**1b**).—The thermal fragmentation of (**1a**) was discovered during an attempt to distill this compound, which resulted in rather violent decomposition at 110 °C. Following this, the behaviour of (**1a**) was studied under more controlled conditions. Monitoring of the progress of the reaction of a mixture of isomers of (**1a**) (*E*:*Z* 55:44) in refluxing benzene by ^{31}P n.m.r. spectroscopy showed gradual disappearance of the *Z* isomer with the concomitant appearance of two new peaks: one at 0.42 p.p.m. (septet), identified as that for dimethyl hydrogen phosphate, and a broad signal at −13.5 p.p.m., which is consistent with a pyrophosphate-type compound and therefore tentatively identified as being due to tetramethyl pyrophosphate[7] (see Table 5). In addition, the formation of benzonitrile was observed, and could be monitored by high-pressure liquid chromatography (h.p.l.c.). Benzonitrile was identified by comparison of its i.r. and n.m.r. spectra and retention time with those of an authentic sample.

In a control experiment the thermal fragmentation of (**1a**) was carried out in the presence of an equimolar amount of dimethyl hydrogen phosphate. In this experiment ^{31}P n.m.r. analysis revealed a considerable increase in the proportion of the signal at −13.5 p.p.m. This is consistent with the assumption regarding the identity of the −13.5 p.p.m. signal as being due to tetramethyl pyrophosphate, which presumably is formed by attack of dimethyl hydrogen phosphate on the phosphorus of (**1a**). On the other hand, heating of dimethyl hydrogen phosphate alone, or with benzonitrile, produced no signal at −13.5 p.p.m.

Examination of Table 5 reveals that in the thermal fragmentation the proportion of (*Z*)-(**1a**) diminishes much more rapidly than that of the *E* isomer. Furthermore the decrease in (*Z*)-(**1a**) can account for most of the products. Therefore it appears that it is the *Z* isomer that selectively undergoes the fragmentation reaction. This conclusion is also supported by the behaviour of the pure *E* compound, which gives products far more sluggishly than the mixture, probably *via* slow equilibration to (*Z*)-(**1a**) that cannot be detected due to its rapid fragmentation. From Table 5 it also appears that the decom-

Table 2. Positional parameters for (*E*)-(**1a**) and (*Z*)-(**1a**). Estimated standard deviations in the least significant digits are shown in parentheses

	(*Z*)-(**1a**)-I			(*Z*)-(**1a**)-II			(*E*)-(**1a**)		
Atom	*x*	*y*	*z*	*x*	*y*	*z*	*x*	*y*	*z*
P	0.333 7(2)	0.375 0(2)	0.944 7(2)	0.287 0(2)	1.161 7(2)	0.084 1(2)	0.902 3(2)	0.119 6(6)	0.7226 (1)
O(1)	0.428 4(6)	0.315 0(4)	1.006 0(5)	0.363 1(6)	0.059 9(5)	1.072 4(5)	0.898 1(5)	0.134 6(2)	0.895 5(4)
O(2)	0.251 3(6)	0.406 3(5)	1.029 8(5)	0.218 8(8)	0.168 2(6)	1.133 0(1)	0.952 7(5)	0.039 9(2)	0.731 8(4)
O(3)	0.388 8(6)	0.442 8(4)	0.889 0(5)	0.359 8(6)	0.092 0(5)	1.260 1(5)	0.051 1(5)	0.159 1(2)	0.678 6(4)
O(4)	0.082 8(7)	0.381 7(5)	0.852 6(7)	0.082 0(6)	0.062 0(5)	1.272 4(7)	0.308 1(5)	0.145 4(2)	0.525 6(4)
N	0.130 0(1)	0.312 4(5)	0.817 0(8)	0.075 0(1)	−0.004 2(6)	1.216 4(7)	0.508 5(5)	0.138 6(2)	0.639 2(5)
C(1)	0.521 0(1)	0.345 9(7)	1.086 3(9)	0.479 4(9)	0.104 3(6)	1.054 6(9)	0.893 4(9)	0.204 5(2)	0.953 9(7)
C(2)	0.195 0(1)	0.489 3(8)	1.030 0(1)	0.136 0(1)	0.200 0(1)	1.081 0(1)	0.824 0(1)	−0.011 6(3)	0.767 1(8)
C(3)	0.247 7(8)	0.302 5(6)	0.859 8(7)	0.171 3(8)	−0.000 3(7)	1.155 0(7)	0.638 9(6)	0.130 2(2)	0.571 5(5)
C(4)	0.305 7(9)	0.225 6(6)	0.821 4(7)	0.178 1(7)	−0.074 5(7)	1.091 5(8)	0.601 8(6)	0.125 8(3)	0.393 4(5)
C(5)	0.432 0(1)	0.225 7(7)	0.801 7(8)	0.183 7(9)	−0.067 7(8)	0.987 1(8)	0.471 8(7)	0.173 5(3)	0.279 8(6)
C(6)	0.485 0(1)	0.155 6(9)	0.764 0(1)	0.190 0(1)	−0.138 0(1)	0.928 0(1)	0.437 6(8)	0.167 8(3)	0.114 4(6)
C(7)	0.417 0(2)	0.085 0(1)	0.749 0(1)	0.191 0(1)	−0.216 0(9)	0.972 0(1)	0.522 0(8)	0.115 5(4)	0.057 3(6)
C(8)	0.293 0(1)	0.083 0(8)	0.766 0(1)	0.183 0(1)	−0.222 6(9)	1.076 0(1)	0.650 0(9)	0.067 2(4)	0.167 3(7)
C(9)	0.235(1)	0.153 0(7)	0.804 8(8)	0.175 7(9)	−0.152 9(8)	1.137 0(1)	0.690 3(8)	0.073 5(3)	0.334 3(6)

Table 3. Important bond lengths and angles for (*E*)-(**1a**) and (*Z*)-(**1a**). Estimated standard deviations in the least significant digits are shown in parentheses

	(*E*)-(**1a**)	(*Z*)-(**1a**)-I	(*Z*)-(**1a**)-II
Bond lengths (Å)			
P–O(1)	1.559(4)	1.564(7)	1.538(8)
P–O(2)	1.566(3)	1.569(7)	1.562(9)
P–O(3)	1.462(4)	1.464(7)	1.447(7)
P–C(3)	1.828(4)	1.801(9)	1.83(1)
O(1)–C(1)	1.444(7)	1.46(1)	1.47(1)
O(2)–C(2)	1.455(8)	1.46(1)	1.18(2)
O(4)–N	1.384(4)	1.32(1)	1.29(1)
N–C(3)	1.284(7)	1.34(1)	1.37(1)
C(3)–C(4)	1.487(7)	1.49(1)	1.46(1)
Bond angles (°)			
O(1)–P–O(2)	102.7(2)	102.4(4)	107.8(6)
O(1)–P–O(3)	116.6(2)	116.1(4)	114.7(4)
O(1)–P–C(3)	106.9(2)	100.9(4)	110.5(4)
O(2)–P–O(3)	110.5(2)	113.4(4)	109.8(6)
O(2)–P–C(3)	107.0(2)	110.8(4)	109.1(5)
O(3)–P–C(3)	112.3(2)	112.3(4)	114.4(4)
P–O(1)–C(1)	122.0(3)	121.6(6)	121.1(7)
P–O(2)–C(2)	121.9(3)	123.6(7)	145.0(1)
O(4)–N–C(3)	113.0(4)	109.0(9)	107.0(9)
P–C(3)–N	112.6(4)	126.0(7)	123.4(8)
P–C(3)–C(4)	118.2(3)	122.5(7)	124.0(6)
N–C(3)–C(4)	129.1(5)	111.3(8)	112.3(9)

Table 4. Important torsion angles for (*E*)-(**1a**) and (*Z*)-(**1a**). Estimated standard deviations in the least significant digits are shown in parentheses

O(3)–P–C(3)–C(4)	44.9(4)	93.0(8)	−113.0(9)
O(2)–P–C(3)–C(4)	−76.5(4)	−138.9(7)	123.5(9)
O(1)–P–C(3)–C(4)	174.0(3)	−31.1(9)	10.3(9)
O(3)–P–C(3)–N	−137.1(3)	−81.4(9)	60.6(1)
O(2)–P–C(3)–N	101.4(4)	46.4(9)	−62.7(1)
O(1)–P–C(3)–N	−8.0(4)	154.2(8)	−175.9(9)
O(1)–P–O(2)–C(2)	57.3(4)	148.0(8)	73.4(2)
O(2)–P–O(1)–C(1)	168.6(4)	−65.6(8)	73.7(9)
O(3)–P–O(1)–C(1)	47.7(4)	58.4(8)	−48.9(8)
C(3)–P–O(1)–C(1)	−78.9(4)	−179.9(7)	−172.1(7)
O(3)–P–O(2)–C(2)	−177.6(4)	22.2(9)	−160.8(2)
C(3)–P–O(2)–C(2)	−55.0(5)	−105.1(8)	−34.8(2)
P–C(3)–N–O(4)	−178.8(3)	−4.2(1)	2.3(1)
C(4)–C(3)–N–O(4)	−1.1(7)	−179.3(8)	176.7(9)
N–C(3)–C(4)–C(5)	46.0(7)	141.1(9)	128.8(1)
P–C(3)–C(4)–C(5)	−136.3(4)	−34.1(1)	−56.8(1)
N–C(3)–C(4)–C(9)	45.3(6)	−38.7(1)	−49.4(1)
P–C(3)–C(4)–C(9)	−132.2(6)	145.9(2)	124.8(1)

Table 5. Thermal fragmentation of 0.8M solution of (**1a**) in refluxing benzene[a]

Time (h)	Starting material (**1a**) % *E*	% *Z*	Products (%) PhCN	Me_2HPO_4	$Me_4P_2O_7$
0	54	46	0	0	0
3	48.5	23.7	n.d.	10.0	17.8
4	48.3	2.9	43	24	24.8
8	42	0	n.d.	31.2	26.5
72	37.9	0	59	35.3	26.8
120	34.1	0	n.d.	44.5	21.4
288	27.8	0	n.d.	49.5	22.7
0	100	0	n.d.	0	0
72	79.5	0	n.d.	20.5	0
288	61.5	0	n.d.	28.2	10.3

[a] The proportions of the phosphorus-containing products were estimated from the integrated signals of ^{31}P n.m.r. The proportion of benzonitrile was determined by high-performance liquid chromatography.

position of (*Z*)-(**1a**) does not obey a simple kinetic equation (compare its quantity after 3 and 4 h). This behaviour might be the result of the influence of the increasing amount of acid (Me_2HPO_4) produced in the reaction, which is expected to change the rate of $Z \longrightarrow E$ isomerization (see next section) as well as, probably, the rate of fragmentation.

The thermal behaviour of oxime ethers (*E*) and (*Z*)-(**1b**) was also examined. Since in this case it was found possible to separate the two geometrical isomers by t.l.c., the two could be investigated separately. The fragmentation of (*Z*)-(**1b**) in refluxing benzene was very slow, but it was possible to bring it to completion in refluxing trimethylbenzene within 72 h. This reaction gave benzonitrile (92%) and trimethyl phosphate (85%) as the only phosphorus-containing product. Isomer (*E*)-(**1b**) was absolutely stable under these conditions.

The results described are consistent with a cyclic mechanism that involves nucleophilic attack by the oxime oxygen on the phosphorus, leading to a 4-membered cyclic intermediate, which then decomposes to products (see Scheme 1). This is consistent with the decreased reaction rate in the oxime ether

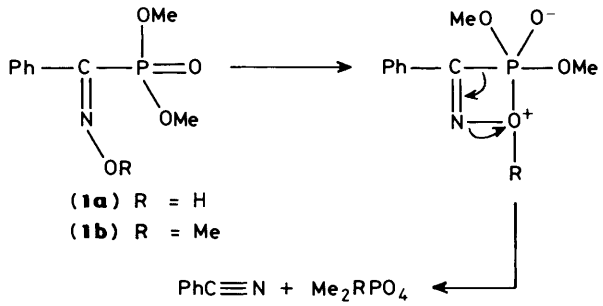

Scheme 1.

(**1b**), as compared with that of the oxime (**1a**), probably as a result of a steric effect.

Alternatively one may assume a pre-equilibrium of (*Z*)-(**1a**) with a zwitterionic intermediate *via* an intramolecularly hydrogen-bonded species (see ref. 1 and calculations in this paper) (Scheme 2), which might facilitate the fragmentation. Such pre-equilibrium is not possible in the case of oxime ether (**1b**).

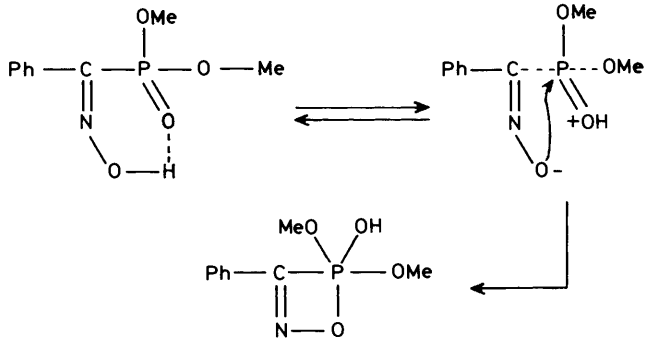

Scheme 2.

The Influence of Acid upon the E–Z *Equilibrium of* (**1**).—We have examined the influence of acid upon the configurational stabilities of oximes (**1a**) and (**1b**). We found by ^{31}P n.m.r. spectroscopy that treatment of mixtures of these compounds (**1a**), (*E*:*Z* 5:4) and (**1b**), (*E*:*Z* 4:6) with methanolic hydrogen chloride catalyses the equilibration of the *E* and *Z* isomers. The equilibrium composition (*E*:*Z* 9:1) is attained in about 7 h both for (**1a**) and (**1b**) in 0.548M hydrogen chloride, while in 3M HCl/MeOH the same requires *ca.* 90 min. This is consistent with what is known regarding the influence of acid upon the isomerization of oximes.[8]

Monode-alkylation of Dimethyl Oxyiminophosphonates (**1**).—Monode-alkylation of the dimethyl esters (**1**) may be achieved by a variety of nucleophiles. Both (**1a**) and (**1b**) underwent de-alkylation by treatment with equimolar amounts of sodium iodide in acetone at room temperature, yielding sodium salts of (**2a**) and (**2b**) without change in the ratio between the *E* and *Z* isomers. Other halides (*e.g.* potassium iodide–acetone or lithium bromide–acetonitrile) could be used as well. In contrast, dealkylation by basic nucleophiles gives solely the more stable *E* isomer of (**2a**). Thus treatment of (**1a**) (*E*:*Z* 5:4) with triethylamine in methanol, or potassium t-butoxide in t-butyl alcohol for 12 h at room temperature, resulted in the quantitative formation of pure (*E*)-(**2a**). In order to find out when the *Z* ⟶ *E* isomerization occurs, we ran a control experiment in which a mixture of the anions (*E* + *Z*)-(**2a**) (*E*:*Z* 5:4) was refluxed for 24 h with a two-fold excess of potassium t-butoxide in t-butyl alcohol. This resulted in recovered starting material with the *E*:*Z* ratio ~6:4. This indicates that the *Z* ⟶ *E* isomerization in the monoanion is very slow, presumably due to the lower ability of the ionized phosphoryl group to stabilize the negative charge at the α position as compared to dimethoxy phosphoryl group in (**1a**), and that most of the *Z* ⟶ *E* isomerization precedes the de-alkylation, presumably by the mechanism indicated in Scheme 3. This

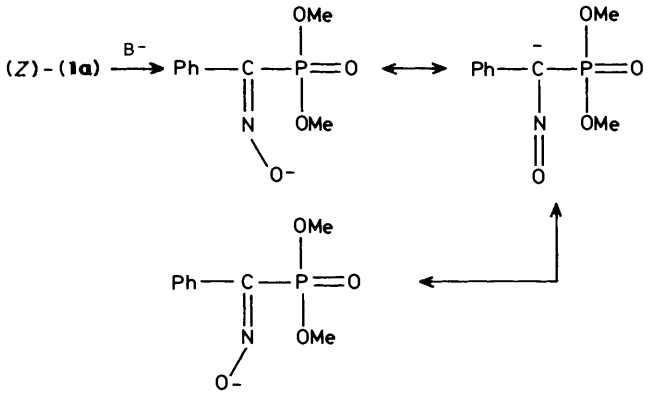

Scheme 3.

conclusion is supported by the lack of isomerization in the reaction of (**1b**) (*E*:*Z* 4:6) with potassium t-butoxide in t-butyl alcohol, which affords (**2b**) in the practically unchanged ratio of *E*:*Z* 46:54. *Z* ⟶ *E* Isomerization cannot take place in this case by the mechanism in Scheme 3 because the oxime function cannot become ionized.

To gain further insight into the modes of interaction of dimethyl esters (**1a**) and (**1b**) with base, their solutions in 0.5M-sodium hydroxide in methanol, at ambient temperature, were examined by ^{31}P n.m.r. spectroscopy. The results listed in Table 6 show that the de-alkylation in oximes (**1a**) is much slower than that in oxime ethers (**1b**).

Among the two geometrical isomers, in the case of (**1a**) only the *E* compound undergoes de-alkylation, while both isomers of (**1b**) react quite rapidly, with (*Z*)-(**1b**) being slightly more reactive than (*E*)-(**1b**). The total lack of reactivity of (*Z*)-(**1a**) in this reaction can be rationalized by assuming electrostatic repulsion of the approaching nucleophile by the ionized oxime hydroxy group which is oriented towards the phosphorus. The lower reactivity of (*E*)-(**1a**) as compared with (*E*)- and (*Z*)-(**1b**) can be explained by assuming the intermediacy of resonance forms that should render the phosphate negatively charged and as a consequence a poorer leaving group (see Scheme 4). The de-

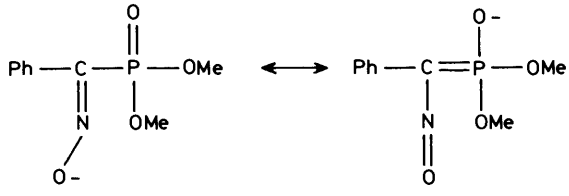

Scheme 4.

alkylation of methyl ethers (*E*)- and (*Z*)-(**1b**) proceeds relatively rapidly and with no isomerization, since in this case there is no interference by an ionizable group.

Monoalkyl α-oxyiminophosphonates (**2**) obtained in the de-alkylation reactions were isolated and characterized as salts. In their i.r. spectrum these compounds show typical P=O bands in the region 1 200—1 210 cm^{-1}, which is significantly lower than

that shown by the dialkyl esters (**1**) (1 240—1 255 cm^{-1}).[9] The methoxy signals of the *E* isomers of salts (**2**), as well as those of the dialkyl esters, appear in the ^1H n.m.r. spectra at lower field than those of the *Z* isomers. In this case, however, the chemical-shift differences between the isomers are larger: $\Delta\delta$ 0.15—0.26 p.p.m. Typical ^{31}P n.m.r. data are presented in Table 1. The higher-field resonances shown by the *Z* isomers both in the ^{31}P and the ^1H n.m.r. spectra are a result of the shielding effect exerted by the non-bonding electrons of the *Z* oriented oxygen upon the phosphorus and the methoxy hydrogens in these compounds.

Acidification of salts (**2**) afforded the free acids; however, these compounds are unstable and undergo fragmentation to benzonitrile and monomeric methyl metaphosphate, which could be trapped by the solvent, as was reported recently.[4] This reaction is applicable for the preparation of unsymmetrical phosphodiesters.

Reaction of (E)- *and* (Z)-(**1a**) *with Sodium Hydroxide.*—In contrast to the de-alkylation reaction that is observed when (**1a**) is treated by bases at room temperature, treatment of (**1a**) with sodium hydroxide at elevated temperatures gives results that depend on the steric structure of the oxime and the reaction medium. The results of these experiments are summarized in Table 7.

From Table 7 it can be seen that the reaction of (**1a**) in aqueous dioxane leads to phosphoric acid, its mono and dimethyl esters, and benzonitrile, while the reaction in alcoholic solvents yields solely de-alkylation products, when the pure *E* isomer is used, and some fragmentation when the mixture is used. The de-alkylation is accompanied by the incorporation of the solvent, which is seen in experiments 5, 6, and 9, which were run in ethanol. The phosphorus compounds were identified by means of their chemical shifts, and the splitting patterns of their ^{31}P n.m.r. phosphorus signals, while benzonitrile was identified on the basis of its spectral properties. On the basis of the results obtained from the reactions of (**2a**) with sodium hydroxide which give methyl dihydrogen phosphate and phosphoric acid (see next section and Table 8), we conclude that methyl dihydrogen phosphate formed in this reaction results from (**2a**) initially formed by de-alkylation (Scheme 5).

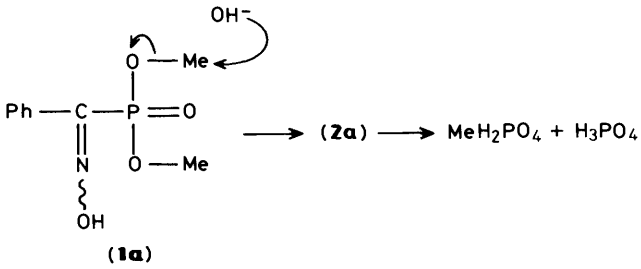

Scheme 5.

In contrast, dimethyl hydrogen phosphate probably comes from fragmentation of the *Z* isomer [(*Z*)-(**1a**)] which is triggered by intramolecular attack of the ionized oxime oxygen upon the phosphorus, as shown in Scheme 6. This assumption is supported: (i) by the differences observed in the product distribution as a function of the geometrical structure of the starting oxime (compare #3 with #4 and #5 with #6 in Table 7). While reactions of the *E*/*Z* mixture give 36—38% dimethyl hydrogen phosphate, the yields of this drop dramatically when the pure *E* isomer is used. The results show that it is the *Z* isomer that leads, *via* C–P bond cleavage, to dimethyl hydrogen phosphate and benzonitrile, while the *E* isomer undergoes predominantly de-alkylation.

(ii) By the results obtained from the treatment of oxime ethers (*E*)- and (*Z*)-(**1b**) under identical conditions. In this experiment both isomers gave products of de-alkylation, but not of C–P bond cleavage, indicating the need for an ionized oxime oxygen for such a reaction.

Consequently it seems reasonable to depict the mode of participation of the oxime hydroxy group in the C–P cleavage *via* a concerted mechanism (Scheme 6).*

In contrast to the *Z* oximes, the phosphorus atom in the *E* isomer (even in the ionized form) is accessible to nucleophilic

Table 6. Reaction of (**1a**) or (**1b**) (0.5M) with sodium hydroxide (0.5M) in methanol at ambient temperature

	(**1a**)		(**2a**)	
Time	*E*%	*Z*%	*W*%	*Z*%
0	54	46	0	0
15 min	62	38	0	0
24 h	48	37	15	0
	(**1b**)		(**2b**)	
0	40	60	0	0
1 h	12	6	24	58

Table 7. Reactions of (**1a**) or (**1b**) (0.125M) with base (0.25M) in different solvents (reflux for 24 h)

No.	Starting material (**1a**) *E*:*Z*	Solvent	Products (%) (*E*)-(**2a**)	Me_2HPO_4	MeH_2PO_4	H_3PO_4	PhCN
1[a]	5:4	20% water in dioxane	0	13	66	21	96
2[a]	1:0	20% water in dioxane	0	8	76	16	n.d.
3[a]	5:4	MeOH	64	36			30
4[a]	1:0	MeOH	91	9			n.d.
5[a]	5:4	EtOH	32[c]	37			n.d.
6[a]	1:0	EtOH	50[c]				0
7[b]	5:4	Bu^{t}OH	92	8			n.d.
	(**1b**) *E*:*Z*		(**2b**) (*E*%:*Z*%)				
8[a]	4:6	MeOH	43:57				0
9[a]	4:6	EtOH	6:12[d]				0

[a] NaOH was used. [b] KOBu^t was used. [c] In reactions 5 and 6 (*E*)-sodium ethyl α-hydroxyiminobenzylphosphonate (*E*)-(**3a**) (31% in 5, and 50% in 6) was also obtained. [d] In reaction 9 38% (*E*)-(**3b**) and 44% (*Z*)-(**3b**) were also obtained. n.d. = not determined.

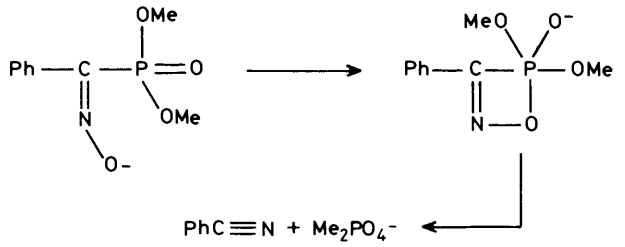

Scheme 6.

attack by the solvent, which may lead to a pentaco-ordinated intermediate as indicated in Scheme 7. The feasibility of this is

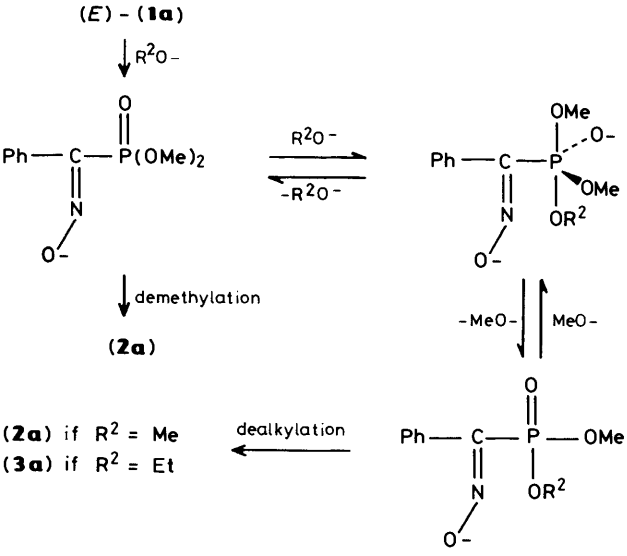

Scheme 7.

also supported by the observation of (*E*)-sodium ethyl α-hydroxyiminobenzylphosphonate (*E*)-(**3a**) in experiments 5 and 6 in Table 7. The final products of (*E*)-(**1a**) under these conditions, (**2a**) and (**3a**), are obtained by nucleophilic de-alkylation.

It is instructive to compare the results from treatment of (**1b**) with base in ethanol (Table 7, # 9 with # 5 in the same table. In the latter the ethyl group was found to be incorporated only to the extent of 50%, and only in the *E* isomer, while in the products from the reaction of the non-ionizable (**1b**) compounds the ethyl group appears in both isomers, to the total extent of 83%. This result emphasizes the increased electrophilicity of the phosphorus in the non-ionizable oxime ethers (**1b**), as compared with the oximes (**1a**). Conversely, however, this also indicates that the phosphorus is significantly electrophilic even in the ionized oxime, (*E*)-(**1**). Apparently, in ionized (*Z*)-(**1a**) nucleophilic attack upon the phosphorus is prevented by the electrostatic repulsion of the *Z* oriented oxide anion, similarly to the prevention of de-alkylation as was discussed in connection with the data in Table 6.

Reactions of (E)- *and* (Z)-(**2a**) *with Sodium Hydroxide.*—The behaviour of monoanions (*E*)- and (*Z*)-(**2a**) was also examined under alkaline conditions. The results are listed in Table 8. Examination of the results listed in this Table reveals that in refluxing aqueous dioxane both isomers of (**2a**) decompose to methyl dihydrogen phosphate and to some phosphoric acid with concomitant formation of benzonitrile in 93% yield.

Under less severe conditions, however, differences in reactivity are seen between the two isomers. Since pure (*E*)-(**2a**) is stable in aqueous solution of sodium hydroxide at room temperature (# 2 in Table 8) as well as in refluxing methanolic sodium hydroxide (# 6), it can be concluded that the methyl dihydrogen phosphate produced in experiments 1 and 5 originates from (*Z*)-(**2a**), presumably through an intramolecular mechanism of the type shown in Scheme 6, for which the ionization of the oxime function is crucial. Indeed, examination of (**2b**) (a mixture of *E* and *Z* isomers), in which the ionization of the oxime function is blocked, under similar conditions (Table 8, # 7) shows complete lack of fragmentation. A similar result was obtained from observation of a solution of (**2b**) in 1M sodium hydroxide solution at room temperature over a period of 8 days, which showed complete stability of both geometrical isomers. These observations provide additional support for the role played by the oxime in the C–P bond fission (Scheme 6).

Further studies show that the oxime (*Z*)-(**2a**) decomposes selectively, slowly when a pH 10 solution of (*E*)- + (*Z*)-(**2a**) is kept at 44 °C. In contrast, solutions of (**2a**) (mixture of *E*:*Z* 55:45 or pure *E*) in borate buffer of pH 9.2 at room temperature showed no change in any respect even after 5 days, indicating that this pH is not sufficiently high to affect either isomerization or fragmentation.

From the data presented it is clear that the chemical properties of α-hydroxyiminophosphonates are determined by the orientation of an ionizable oxime OH group. In cases when this group is ionized, and *Z* oriented with respect to the phosphorus, it promotes fragmentation of the molecule by cleavage of the C–P bond, and it blocks attack by anions at the phosphorus and at the P–O–alkyl groups. This is in contrast to *E* oximes, which behave quite normally. From a practical standpoint our results may be summarized by saying that compounds of type (*Z*)-(**2**) are stable, and can be used in the pH range of ~7—9, while the *E* isomers are stable at room temperature up to pH ~14.

Molecular Structure

Theoretical Calculations.—We calculated the structures of dimethyl oxyiminophosphonates (*Z*)-(**1a**) and (*E*)-(**1a**). Table 9 presents the energies of the optimized structures for both the full optimizations and those constrained by the crystallographic torsion angles. For the oxime (*Z*)-(**1a**) a few local minima were found, two of which have internal hydrogen bonding which stabilizes the structure. In Table 10 we compare the structural features of the calculated and crystallographically determined structures.

Based on results from calculations performed on benzoylphosphonates,[10] optimization of the oximes was initiated with an *s-trans* alignment for C=N and P=O about the C–P bond. The low rotation barrier and the small enthalpy difference between *s-cis* and *s-trans* in benzoylphosphonate may be even lower in the oxime (*Z*)-(**1a**) due to the possibility of internal H-bonding for the *s-cis* conformation. However, other possible

* Analogous fragmentation was noted in the case of α-hydroxyiminoalkyltriphenylphosphonium bromides, which were found to yield, under the influence of base, triphenylphosphine oxide and a nitrile. In this case, however, the geometry of the oximes was not determined and therefore the stereoselectivity of the reaction is not known: S. Trippett, B. J. Walker, and H. Hoffmann, *J. Chem. Soc.*, 1965, 7140. Intramolecular interaction between an oxime and a phosphoryl group has also been noted in cases where the distance between the functional groups is greater, and the interaction lends assistance to phosphonate hydrolysis *via* 5-membered intermediates: J. I. G. Cadogan, D. T. Eastlick, J. A. Challis, and A. Cooper, *J. Chem. Soc., Perkin Trans. 2*, 1973, 1798; P. Livant and M. Cocivera, *J. Org. Chem.*, 1978, **43**, 3011.

Table 8. Reactions of (**2a**)·Na^+ or (**2b**)·Na^+ (0.125M) with sodium hydroxide in different solvents

No.	Starting material (**2a**) *E*:*Z*	Solvent	Products (%) PhC≡N	(**2a**)	*E*:*Z*	MeH_2PO_4	H_3PO_4
1[a]	55:45	water	18	84	56:28	16	0
2[a]	100:0	water	n.d.	100	100:0		0
3[b]	55:45	20% water	93	0	0	92	8
4[b]	100:0	in dioxane	n.d.	0	0	88	12
5[b]	55:45	MeOH	n.d.	80	47:33	20	0
6[b]	100:0	MeOH	0	100	100:0	0	0
	(**2b**) *E*:*Z*			(**2b**)	*E*:*Z*		
7[b]	45:55	MeOH	0	100	47:53		

Conditions: [a] 1M NaOH, 36 h, 25 °C. [b] 0.125M NaOH, 24 h, reflux. n.d. = not determined.

Table 9. Calculated heats of formation for oxime derivatives in the gas phase and crystal[a]

Structure	Identification	ΔH_f/kcal mol^{-1}	H-bonds	G = Gas phase X = *X*-Ray
1	(*Z*)-(**1a**)	−117.94	N–O–H- - -O=P	G
2	(*Z*)-(**1a**)-I	−107.77		X
3	(*Z*)-(**1a**)-II	−101.84		X
4	(*E*)-(**1a**)	−115.58		G
5	(*E*)-(**1a**)	−109.05		X

[a] In calculations based on crystal structures (2, 3, 5) the 'best' directions of hydrogens were chosen by geometry-minimization procedures.

Table 10. Comparison of calculated and crystallographically determined parameters of (*Z*)-(**1a**)[a]

Geometric parameter	*X*-Ray		Calculation
Bond length			
N–C(3)	1.344	1.366	1.315
C(3)–P	1.801	1.832	1.787
P–O(3)	1.464	1.447	1.524
P–O(1)	1.564	1.538	1.608
C(1)–O(1)	1.460	1.473	1.392
C(2)–O(2)	1.463	1.177	1.393
C(4)–C(3)	1.489	1.456	1.468
C(4)–C(9)	1.397	1.390	1.417
O(4)–N	1.322	1.290	1.266
Bond angle			
N–C(3)–P	126.0	123.4	118.1
C(3)–P–O(3)	112.3	114.4	107.2
C(3)–P–O(1)	100.9	100.5	110.5
C(3)–P–O(2)	110.8	109.1	109.4
P–O(1)–C(1)	121.8	121.1	125.9
P–O(2)–C(2)	121.6	145.0	125.8
C(3)–C(4)–C(9)	123.6	119.5	120.6
C(3)–N–O(4)	120.2	107.0	124.3
	109.0		
Torsion angle			
N–C(3)–P–O(3)	−81.49	60.65	0.5
N–C(3)–P–O(1)	154.27	−175.92	−124.7
N–C(3)–P–O(2)	46.45	−62.76	122.6
O(3)–P–O(1)–C(1)	58.44	−48.98	8.0
O(3)–P–O(2)–C(2)	22.21	−160.88	−31.2
C(9)–C(4)–C(3)–N	−38.77	−49.48	−90.0

[a] Comparison is with structure I of the *X*-ray determination.

contributions of H-bonding to phosphoryl oxygens could modify the barrier and must be considered in assessing the conformers' populations.

I. (Z)-*Dimethyl α-hydroxyiminobenzylphosphonate* (*Z*)-(**1a**). The global optimum found for the oxime (*Z*)-(**1a**) is shown in Figure 3. It has a hydrogen bond between the oxygens of the oxime and phosphoryl functions. The existence of such a bond is evident from the atom–atom bond-density matrix. The density

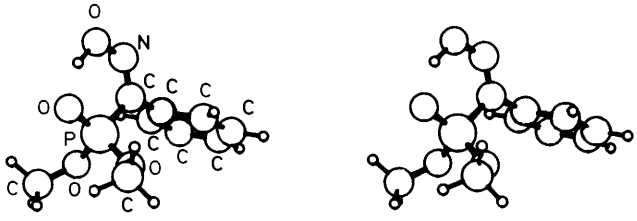

Figure 3. Stereo plot of the 'gas-phase' hydrogen-bonded optimal structure of oxime (*Z*)-(**1a**)

between the acceptor phosphoryl oxygen and the donor hydroxy proton is 0.589 (distance of 1.488 Å), while the antibonding density among the two oxygens involved is −0.0069 (*R* 2.417 Å). Those are values which were previously found to be characteristic of H-bonding.[11] The stabilization conferred by the H-bond becomes evident when the proton's position is 'forced' to rotate from its optimal H-bonding arrangement. Some 6.1 kcal are lost when it is rotated to an '*anti*' direction with respect to the phosphoryl oxygen. As the rotation about the C–P bond without H-bonding requires similar energy to the one found for dimethyl benzoylphosphonate (*i.e.*, 1.8 kcal),[10] the gain of stabilization by H-bonding is estimated to be about 2.0 kcal. Other conformations may be populated as well in the 'gas-phase' molecule. Rotation about the C–P bond is not energetically expensive and may lead to other internal H-bonded conformers. The next accessible conformation has an internal H-bond to one of the methoxy oxygens, but its energy is some 2.8 kcal above the minimum, and the H-bond is weaker, as judged by the bond-density matrix. This is a result of the different geometry of the H-bond: while the

O---O distance is nearly unchanged, compared with the global minimum (*R* 2.496 Å, *vs.* *R* 2.417 Å), a longer H---O(Me) distance is found here (*R* 1.608 Å *vs.* *R* 1.489 Å). As a result, the O–H---O angle becomes smaller in the less stable H-bond.

II. (E)-*Dimethyl α-hydroxyiminobenzylphosphonate* (*E*)-(**1a**). The oxime (*E*)-(**1a**) shows some deviations between calculated and *X*-ray geometry parameters comparable to those found for the *Z* isomer. The global optimum is lower by 6.5 kcal mol^{-1} than the calculated optimum which was restricted by the *X*-ray torsion angles. There is a large difference in the calculated dipole moments of those two structures: 1.96*D* for the gas-phase global optimum, and 4.82*D* for the restricted optimum. We assume that in a non-polar medium the molecule should prefer a conformation with a lower dipole moment, if it is energetically accessible. The direction of the dipole calculated for the *X*-ray structure is superimposed on the molecule in Figure 4. In the

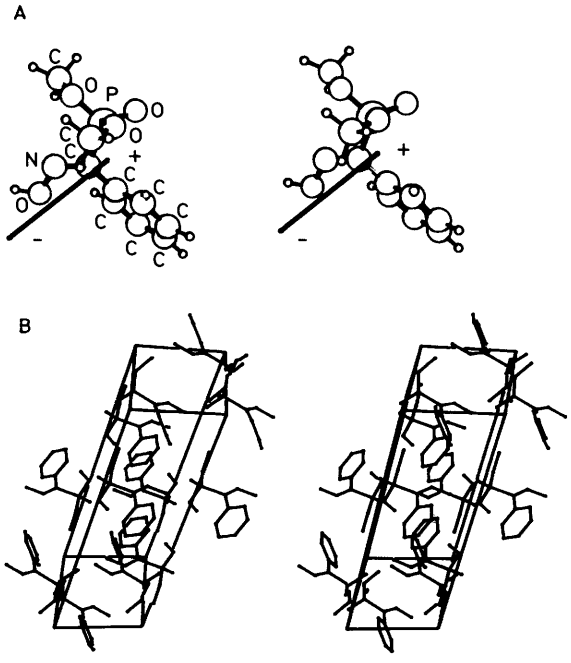

Figure 4. A. Stereo plot of the *X*-ray conformer of oxime (*E*)-(**1a**) with the calculated direction of its dipole. B. The unit cell of oxime (*E*)-(**1a**)

same figure, the cell structure of the *E*-oxime crystal is given. The packing is in 'layers,' whereas the dipole direction, shown for the individual *E*-oxime, is parallel within one layer, and nearly anti-parallel in the two neighbouring layers, below and above any given layer. This may be seen more clearly in the two central layers of the cell. Thus we have good reason to believe that the gas-phase optimum for the *E*-oxime may be the one preferred also in non-polar solvents, while in the crystal the molecules adopt a different conformation, higher in energy than their 'ground state,' due to the efficiency of packing in an electrostatically more favourable environment.

X-*Ray Crystallography*.—The molecular structures are depicted in Figures 1 and 2. The bond lengths, bond angles, and torsion angles all fall within a reasonable range expected for similar compounds. There are, however, several structural features which should be pointed out. The most interesting feature is the geometry around the C(3) atom in the (*E*)-(**1a**) *vs.* (*Z*)-(**1a**) structures. The sp^2-hybridization of the C(3) atom is expected to result in bond angles of ~120° around it. A close inspection of the bond lengths and bond angles (see Table 3) reveals that the P–C(3)–N angle in the *E* isomer (112.6°) is significantly lower than the corresponding angles in the *Z* isomers (126.0° and 123.4°). Also the C(3)=N [1.284 Å in (*E*)-(**1a**), and 1.34 Å in (*Z*)-(**1a**)] and the N–O [1.384 Å in (*E*)-(**1a**), and 1.32 Å in (*Z*)-(**1a**)] bond lengths display interesting differences (Table 3).

These results seem to indicate that there is steric crowding between the oxime OH moiety and the phosphorus oxygen atoms in the *Z* isomer, and between the oxime OH and the phenyl ring in the *E* isomer. The geometrical dispositions seem to be a result of an attempt to relieve the steric crowding. In the *Z* isomer the OH---O(3) distance is 2.83 Å in (*Z*)-(**1a**)-I, while the corresponding constants in (*Z*-(**1a**)-II are 2.98 Å [OHA---O(2)A] and 3.04 Å [OHA---O(3)A]. These differences could arise from a rotation around the P–C(3) bond. While the existence of a weak hydrogen bond cannot be ruled out entirely, it is safe to say that no hydrogen bonds exist in (*Z*)-(**1a**)-II.

An inspection of the unit-cell packing revealed that despite the existence of phenyl rings no stacking interactions were observed. We have observed intermolecular hydrogen-bonding contacts between OH---O(3)A and OHA---O(3) (2.69 Å). The network of the hydrogen bonds affects the packing and could explain the differences observed between the two crystallographically independent molecules, and between them and the gas-phase calculations.

Despite the differences between the calculated and the *X*-ray structures of (*Z*)-(**1a**), the internal ordering of the bond lengths and bond angles reflects great similarity between the two structures. The deviations in torsion angles may be due to the packing forces. The calculation finds the phenyl ring out of the plane of N=C–P, which is also observed in both molecules in the crystal structure, albeit at a different angle.

Both the calculations and the crystal-structure analyses reveal that there is a fair amount of conformational flexibility, which should be manifested in the solution structures of the molecules.

Experimental

All m.p.s were determined by a Thomas-Hoover capillary melting-point apparatus and are uncorrected. Elemental analyses were performed by the Analytical Laboratories, Givat-Ram, The Hebrew University, Jerusalem. I.r. spectra were determined on a Perkin-Elmer Model 457 spectrophotometer. Nuclear magnetic resonance spectra were obtained on a Varian XL-100 or a Bruker-WH-300 instrument, ^{1}H and ^{31}P spectra being recorded in deuteriochloroform or in deuterium oxide solutions. Chemical shifts are reported in p.p.m. from $SiMe_4$ or $Me_3SiC^2H_2C^2H_2CO_2Na$ as internal standard in ^{1}H spectra and from 85% H_3PO_4 as external standard in ^{31}P spectra; positive chemical shifts are to low field with respect to the standard. High-pressure liquid chromatography (h.p.l.c.) was carried out using a Merck-Hitachi instrument with an Rp-18 column. Gas chromatographic work was carried out with a Varian model 1400 gas chromatograph equipped with a copper tube (1.5 m × $\frac{1}{4}$ in O.D.) packed with 10% Carbowax 20M on Chromosorb W 60—80; peak areas were determined by the internal-standard method.

Materials.—Trimethyl, triethyl, and tributyl phosphites, hydroxylamine hydrochloride, *O*-methylhydroxylamine hydrochloride, and the acyl chlorides, with the exception of lauroyl chloride, were obtained from Aldrich Chemical Company. Lauroyl chloride was prepared by treatment of pure lauric acid with an excess of thionyl chloride. Other common reagents were obtained commercially in high purity.

General Method for the Synthesis of Dialkyl Acylphosphonates.—(A modification of that described by Kabachnik.[12]) Trialkyl phosphite (0.2 mol) was added dropwise to the acyl chloride (0.2 mol) at 5 °C. After the addition was complete, the reaction mixture was stirred for 1 h at the ambient temperature. The products were isolated by low-pressure distillation in yields of 75—90%.

General Method for the Synthesis of α-Oxyiminophosphonates.—Dialkyl acylphosphonate (0.1 mol) was added slowly to a solution of hydroxylamine hydrochloride or of *O*-methylhydroxylamine hydrochloride (0.11 mol) and pyridine (0.12 mol) in absolute methanol (100 ml). The reaction mixture was stirred for 72 h. Evaporation of the methanol under reduced pressure gave a syrup, which was mixed with 1M HCl (50 ml). The aqueous mixture was extracted with chloroform (4 × 75 ml), and the combined extracts were washed with water (100 ml), dried over anhydrous magnesium sulphate, filtered, and evaporated, to yield the product (**1**) and (**4**)—(**10**) (80—90%), which was subjected to ^{1}H and ^{31}P n.m.r., and i.r., spectroscopy as well as elemental analysis. ^{31}P Chemical shifts are listed below.

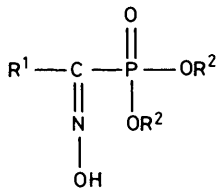

Oxime derivatives	^{31}P chemical shifts (p.p.m.)
(**4**) $R^1 = R^2 = Me$	(*E*:*Z* = 4:1) δ_E 11.90, δ_Z 6.80
(**5**) R^1 = n-C_6H_{13}, R^2 = Me	(*E*:*Z* = 9:1) δ_E 12.37, δ_Z 7.69
(**6**) R^1 = n-$C_{11}H_{23}$, R^2 = Me	(*E*:*Z* = 4:1) δ_E 12.31, δ_Z 7.66
(**7**) R^1 = Ph, R^2 = Bu	(*E*:*Z* = 77:23) δ_E 8.01, δ_Z 3.59
(**8**) R^1 = 4-ClC_6H_4, R^2 = Me	(*E*:*Z* = 4:1) δ_E 12.12, δ_Z 8.71
(**9**) R^1 = 4-$MeOC_6H_4$, R^2 = Me	(*E*:*Z* = 19:1) δ_E 13.01, δ_Z 8.63
(**10**) R^1 = Ph, R^2 = Et	(*E*:*Z* = 7:3) δ_E 7.74, δ_Z 3.27

Separation of (E)- *and* (Z)-*Dimethyl α-Methoxyiminobenzylphosphonate* (E)- *and* (*Z*)-(**1b**).—The two isomers were separated by preparative t.l.c. Chromatograms on glass plates (20 × 20 cm) coated with silica gel (GF_{254}, 1 mm thickness) were developed by ethyl acetate. The two products: (*E*)-(**1b**) (lower band) and (*Z*)-(**1b**) (higher band), both oils, were isolated by extraction with chloroform, and were characterized by n.m.r. spectroscopy.

Acid-catalysed Isomerization of (E)- *and* (Z)-*Dimethyl α-Hydroxyiminobenzylphosphonate* (E)- *and* (Z)-(**1a**).—A mixture of (*E*)-(**1a**) and (*Z*)-(**1a**) (*E*:*z* 55:44) (458 mg, 2 mmol) was dissolved in methanolic hydrogen chloride (4 ml; 0.548M). After filtration to remove the precipitated sodium chloride, the solution was monitored by ^{31}P n.m.r. spectroscopy. The same procedure was repeated with a mixture of (*E*)-(**1a**) and (*Z*)-(**1a**) (458 mg, 2 mmol) and a solution of 3M methanolic hydrogen chloride (4 ml).

Synthesis of (E)-*Dimethyl α-Hydroxyiminobenzylphosphonate* (E)-(**1a**).—A mixture of (*E*)- and (*Z*)-(**1a**) (*E*:*z* 55:44) (22.9 g, 0.1 mol) was dissolved in 3M methanolic hydrogen chloride (75 ml). The reaction mixture was stirred for 5 h at ambient temperature. The methanol was evaporated off and the residue (22.5 g) was crystallized from benzene, yielding white crystals of (*E*)-(**1a**) (18.5 g, 80%), m.p. 101 °C.

Thermal Fragmentation of Dimethyl α-Hydroxyiminobenzylphosphonate (E)- *and* (Z)-(**1a**).—A mixture of (*E*)- and (*Z*)-(**1a**) (*E*:*Z* 55:44) (446 mg, 3.2 mmol) was dissolved in dry benzene (4 ml). The reaction mixture was heated to 80 °C and monitored by ^{31}P n.m.r. spectroscopy and h.p.l.c. The results are summarized in Table 5. The reaction was repeated with the same mixture (22.9 g, 0.1 mol) and dry benzene (100 ml). The reaction mixture was refluxed for 72 h. The benzene was evaporated off and the oily residue was triturated with hexane (4 × 50 ml). The combined hexane layers were evaporated and the residue was distilled to yield benzonitrile, b.p. 188 °C (lit.,[13] 188 °C) (6 g, 58%), which was identified by comparison of its i.r. and n.m.r. spectra to those of an authentic sample. The residue, which did not dissolve in hexane, was dissolved in chloroform and the solution was evaporated after filtration. The oily residue was analysed by ^{31}P n.m.r. spectroscopy. The results obtained indicated that the mixture contained (*E*)-(**1a**), dimethyl hydrogen phosphate, and an unidentified phosphorus-containing product (δ_P − 13.5 p.p.m.) in the proportions 7:7:5, on the basis of their signal areas.

Thermal Fragmentation of (Z)-*Dimethyl α-Methoxyiminobenzylphosphonate* (Z)-(**1b**).—(*Z*)-(**1b**) (1.22 g, 5 mmol) was dissolved in 1,2,4-trimethylbenzene (10 ml) and the reaction mixture was refluxed for 72 h. The ^{31}P n.m.r. spectrum of the cooled solution showed only one peak, at 0.6 p.p.m., which was found to be identical with that of trimethyl phosphate. The reaction was repeated with (*Z*)-(**1b**) (1.22 g, 5 mmol) which was heated in the neat form at 140 °C for 30 min. The product mixture was analysed by i.r., ^{1}H n.m.r., and ^{31}P n.m.r. spectroscopy and by gas chromatography which indicated the presence of benzonitrile (0.48 g, 92%) and trimethyl phosphate (0.46 g, 85%).

General Procedure for De-alkylation of Dialkyl α-Oxyiminophosphonates.—To a dry solution of dialkyl α-oxyiminophosphonate (0.1M in 100 ml) was added the dry reagent 1.1 mol equiv) LiBr, NaI, KI, Et_3N, or Bu^{t}OK and the reaction mixture was stirred for 12 h at ambient temperature. The white precipitate obtained was filtered off, washed with dry acetone (50 ml), and dried, yielding the product (70—96%), which was subjected to ^{1}H n.m.r., i.r., and elemental analysis (Table 11). The mixture of isomers was analysed in the case of compound (**2a**) by h.p.l.c. on a Hypersil 50 ODS RP column, with a mobile phase of 5% acetonitrile in 25 mM triethylamine–acetic acid buffer of pH 6.5. At a flow rate of 1.1 ml min^{-1} (*E*)-(**2a**) had R_t ~ 11 min, while (*Z*)-(**2a**) had R_t ~ 16 min. ^{31}P Chemical shifts are listed below.

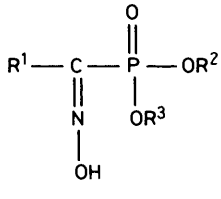

Oxime derivatives	^{31}P chemical shifts (p.p.m.)
(**3a**) Li R^1 = Ph, R^2 = Et, R^3 = Li	(1 isomer) δ 5.70
(**11**) $R^1 = R^2$ = Me, R^3 = Li	(1 isomer) δ 9.85
(**12**) R^1 = n-C_6H_{13}, R^2 = Me, R^3 = Li	(1 isomer) δ 9.73
(**13**) R^1 = n-$C_{11}H_{23}$, R^2 = Me, R^3 = Li	(1 isomer) δ 10.17
(**14**) R^1 = Ph, R^2 = Bu, R^3 = Li	(*E*:*Z* 19:1) δ_E 6.02, δ_Z 2.21
(**15**) R^1 = 4-ClC_6H_4, R^2 = Me, R^3 = Na	(*E*:*Z* 3:2) δ_E 7.22, δ_Z 3.02
(**16**) R^1 = 4-$MeOC_6H_4$, R^2 = Me, R^3 = Na	(*E*:*Z* 3:2) δ_E 7.95, δ_Z 3.75

Table 11. Analytical data of products from mono-de-alkylation reaction of dialkyl oxyiminophosphonates

Compound	De-alkylation reagent	Formula	Elemental analysis Calculated (%) C	Calculated (%) H	Found (%) C	Found (%) H
(2a)[a]	NaI	$C_8H_9NNaO_4P$	40.51	3.80	40.25	3.75
(11)	LiBr	$C_3H_7LiNO_4P$	22.64	4.40	22.6	4.4
(12)	LiBr	$C_8H_{17}LiNO_4$	41.92	7.42	41.2	7.5
(13)	LiBr	$C_3H_{17}LiNO_4$	52.17	9.03	52.4	9.1
(2b)	NaI	$C_9H_{11}NNaO_4P$	43.03	4.38	42.9	4.35

[a] Salts of **(2a)** with other cations were identified on the basis of their identical spectra to that of **(2a)**-Na^+

General Procedure for the Reactions of Dimethyl α-Hydroxyiminobenzylphosphonate **(1a)** *and Dimethyl α-Methoxyiminobenzylphosphonate* **(1b)** *with Bases.*—Substrate **(1a)** or **(1b)** (0.01 mol) and a base (0.02 mol) (see Table 7) were dissolved in a solvent (80 ml) (Table 7). The reaction mixture was refluxed for 24 h, the solvent was evaporated, and the residue was analysed (^{31}P n.m.r. and h.p.l.c.). The results obtained are summarized in Table 7. The quantities of benzonitrile were determined by h.p.l.c. and of the phosphorus-containing products were calculated from the peak areas of the ^{31}P n.m.r. spectra.

General Procedure for the Reactions of Sodium Methyl α-Hydroxyiminobenzylphosphonate **(2a)** *and Sodium Methyl α-Methoxyiminobenzylphosphonate* **(2b)** *with Bases.*—Substrate **(2a)** or **(2b)** (0.01 mol) and a base (0.02 mol) were dissolved in a solvent (80 ml) (Table 8). The reaction mixture was refluxed for 24 h. The solvent was evaporated off and the residue was analysed (^{31}P n.m.r. and h.p.l.c.). The quantities of benzonitrile were determined by h.p.l.c. and of the phosphorus-containing products were calculated from the peak areas of the ^{31}P n.m.r. spectra.

Crystallizations.—*X*-Ray-quality crystals of the *E* and *Z* isomers of **(1a)** were obtained by slow evaporation from a benzene solution. The crystals were large and well formed.

Data Collection and Processing.—The crystals were mounted on glass fibres using epoxy resin. Data sets were collected on a PW 1100 Philips four-circle computer-controlled diffractometer. Mo-K_α (λ 0.710 69 Å) radiation with a graphite crystal monochromator in the incident beam was used. Unit-cell parameters were obtained by a least-squares fit of 25 high-angle reflections ($13 < \theta < 16°$). The data sets were collected in the θ–2θ scan mode. The scan width, *w*, for each reflection was 1° with a scan time of 20 s. Background measurements were made at both limits of each scan. For each data set Lorentz and polarization corrections were applied. None of the data sets displayed any decay in the intensities of the standard reflections and no correction was applied. No absorption correction was applied. Other information pertinent to data collection and processing is given in Table 12.

Structure Analysis and Refinement.—In both structures the co-ordinates of the phosphorus atoms were obtained by the direct programs MULTAN and SHELX-86.[14] The positions of the remaining non-hydrogen atoms were obtained from subsequent refinements and difference Fourier maps. Anisotropic thermal parameters were used for all phosphorus, nitrogen, oxygen, and carbon atoms of both structures. The aromatic hydrogen atoms were placed in their calculated positions, were constrained to 'ride' on the carbon atoms, and were refined using common thermal parameters. For both structures (*Z*)- and (*E*)-**(1a)** the methyl hydrogens were placed in their calculated positions and refined using a group thermal parameter.

Table 12. Crystallographic data for (*E*)-**(1a)**, (*Z*)-**(1a)**, and (*E*)-**(2b)**

	(*E*)-**(1a)**	(*Z*)-**(1a)**	(*E*)-**(2b)**
Elem. formula	$C_9H_{12}NO_4P$	$C_9H_{12}NO_4P$	$C_9H_{11}NNaO_4P$
Mol. weight	229	229	251
Space group	$P2_1/c$	$P2_1/n$	$P2_1/c$
a (Å)	7.046(1)	10.717(1)	16.130(2)
b (Å)	19.217(2)	16.031(2)	7.045(1)
c (Å)	8.793(1)	13.090(1)	13.212(1)
β (°)	112.80()	95.43(1)	110.51(1)
V (Å^3)	1 097(1)	2 239(1)	1 406(1)
D (calc.) (g cm^{-3})	1.3864	1.3586	1.857
Z	4	8	4
μ (cm^{-1})	1.96	1.93	2.02
Range of 2θ (°)	4—45	4—46	4—45
No. of unique data	1 913	3 158	2 456
No. of data with $F_o^2 > 3\sigma(F_o^2)$	1 428	2 141	2 184
R_1[a]	0.0553	0.090	0.0578
R_2[a]	0.0585	0.0912	0.0645

[a] $R_1 = |\Sigma|F_o| - |F_c||/\Sigma|F_o|$ $R^2 = [\Sigma w(|F_o| - |F_c|)^2/\Sigma|F_o|^2]^{1/2}$

Using SHELX-76,[15] full-matrix, least squares refinements were carried out on 144 and 273 variables for structures (*E*)-**(1a)** and (*Z*)-**(1)** respectively. The refinements, using unit weights, converged to reasonable discrepancy factors which are listed in Table 12.

Final non-hydrogen positional parameters, together with their estimated standard deviations, for both structures, appear in Table 2. Important interatomic distances, together with their standard deviations, are given in Table 3. Important bond angles, with their standard deviations are given in Table 3 and torsion angles are listed in Table 4.*

Figure 1 depicts a labelling scheme of (*E*)-**(1a)**, and figure 2 depicts the molecular geometry and labelling scheme of (*Z*)-**(1a)** (one molecule).

Methods of Calculation.—Semiempirical SCF calculations were carried out by MNDO/H,[11] which is an improved version of the original MNDO,[16] modified to describe properly any multiply H-bonded systems.[17] Total geometry optimization with gradient analytical derivatives[18] was used throughout.

* *Supplementary data* (see section 5.6.3 of Instructions for Authors, in the January issue). Listings of anisotropic thermal parameters, positional and thermal parameters of the hydrogen atoms, and the bond lengths, bond angles, and torsion angles of the phenyl rings have been deposited at the Cambridge Crystallographic Data Centre.

Rotation barriers were evaluated by the reaction co-ordinate technique,[19] limiting the values of rotation for the appropriate degree of freedom while optimizing all other variables.

Comparisons with crystallographic results were made by imposing the rotational angles on those found in the *X*-ray structures, while optimizing all bond lengths and angles. This is required in order to remain within the given limits of the semi-empirical study.

Owing to the potential for hydrogen bonding in (*Z*)-(**1a**), we investigated a few conformations which had an initial geometry enabling the formation of H-bonds among the oxime oxygen and one (single H-bond) or two (bifurcated H-bond) of the phosphoryl oxygens. All the calculations are of the 'gas phase' type and did not include any simulation or representation of the solvent.

Acknowledgements

This research was supported, in part, by a grant from the United States–Israel Binational Science Foundation (B.S.F.), Jerusalem, Israel (to E. B.), and in part by a grant from the Joint Research Fund of the Hebrew University and Hadassah (to D. G.). B. V. L. P. is a Lister Institute Fellow.

References

1 K. D. Berlin, R. T. Claunch, and E. T. Gaudy, *J. Org. Chem.*, 1968, **33**, 3090.
2 Yu. A. Zhdanov, L. A. Uzlova, and Z. I. Glebova, *Russ. Chem. Rev. (Engl. Transl.)*, 1980, **49**, 843.
3 K. D. Berlin, N. K. Roy, R. T. Claunch, and D. Bude, *J. Am. Chem. Soc.*, 1968, **90**, 4494; J. Kowalik, L. Kapczyk-Subotkowska, and P. Mastalerz, *Synthesis*, 1981, 57; D. Redmore, in 'Topics in Phosphorus Chemistry,' eds. M. Grayson and J. Griffith, Interscience, New York, 1976, vol. 8, pp. 515—585.
4 E. Breuer, R. Karaman, H. Leader, and A. Goldblum, *J. Chem. Soc., Chem. Commun.*, 1987, 671.
5 E. Breuer, R. Karaman, D. Gibson, H. Leader, and A. Goldblum, *J. Chem. Soc., Chem. Commun.*, 1988, 504.
6 G. Geiseler, and G. Muller, *Spectrochim. Acta*, 1973, **29A**, 345.
7 V. Mark, C. H. Dungan, M. M. Crutchfield, and J. R. Van Wazer, in 'Topics in Phosphorus Chemistry,' eds. M. Grayson and J. Griffith, Interscience, New York, 1967, vol. 5, p. 331.
8 C. R. Hauser, and D. S. Hoffenberg, *J. Org. Chem.*, 1955, **20**, 1491.
9 L. S. Bellamy, 'The Infrared Spectra of Complex Molecules,' Methuen & Co., London, 2nd ed., 1959, p. 311; D. E. C. Corbridge, in 'Topics in Phosphorus Chemistry,' eds. M. Grayson and J. Griffith, Interscience, New York, 1969, vol. 6, pp. 235—365.
10 R. Karaman, A. Goldblum, H. Leader, and E. Breuer, *J. Chem. Soc., Perkin Trans 1*, 1988, in the press.
11 A. Goldblum, *J. Comput. Chem.*, 1987, **8**, 835.
12 M. I. Kabachnik and P. A. Rossiskaya, *Izv. Akad. Nauk. SSSR, Otd. Khim. Nauk.*, 1945, 364; K. D. Berlin and H. A. Taylor, *J. Am. Chem. Soc.*, 1964, **86**, 3862.
13 Beilsteins Handbuch der Organischen Chemie, vol. IX, p. 275.
14 P. Main, S. E. Hull, L. Lessinger, G. Germain, J. P. Declercq, and M. M. Woolfsoon, 'MULTAN 78,' University of York, 1978.
15 G. M. Sheldrick, SHELX-76: in 'Computing in Crystallography,' eds. H. Schenck, R. Olthof-Hazekamp, H. van Koningsveld, and G. C. Bassi, Delft University Press, Delft, 1978, pp. 34—42.
16 K. Ya. Burstein and A. N. Isaev, *Theor. Chim. Acta*, 1984, **64**, 397.
17 A. Goldblum and G. H. Loew, *J. Am. Chem. Soc.*, 1985, **107**, 4265.
18 M. C. Flanigan, A. Komornicki and J. W. McIver, Jr., in 'Modern Theoretical Chemistry,' ed. G. A. Segal, Plenum Press, New York, 1977, vol. 8.
19 G. P. Ford and J. D. Scribner, *J. Comput. Chem.*, 1983, **4**, 594.

Received 9*th February* 1988; *Paper* 8/00429C